ELSEVIER

Biochimica et Biophysica Acta 1370 (1998) 235–242

BIOCHIMICA ET BIOPHYSICA ACTA
BBA

Quantification of concanavalin A binding to rat brain microsomal membranes detected by fluorescence polarization technique

M. Miyazaki [a,b], S. Yoshida [a,*], K. Sakai [a], Q.Z. Zhang [a], M. Takeshita [b]

[a] *Research Laboratory Center, Oita Medical University, Hasama-cho, Oita 879-55, Japan*
[b] *Department of Biochemistry, Oita Medical University, Hasama-cho, Oita 879-55, Japan*

Received 8 September 1997; accepted 31 October 1997

Abstract

A high sensitive method for detecting the change of microsomal membrane surface oligosaccharides was developed to study the regulatory role of lipid- or peptide-linked mannoside of endoplasmic reticulum in synaptic functions. The binding of concanavalin A to the microsomal membrane surface was measured quantitatively using a microgram-order of rat brain microsomal proteins. The fluorescence polarization of concanavalin A (Con A)-fluorescein isothiocyanate (FITC) conjugate bound to the membrane was analyzed to quantitate the change of binding constant and the number of binding sites. As a control, the non-specific binding of bovine serum albumin–FITC conjugate was measured by the same technique. We measured the change of fluorescence intensity of membrane-bound FITC conjugates by the flow cytometry and found that the intensity of FITC conjugate bound to the membrane increased more than that of free form of the probe. We observed that the alpha-mannosidase-treatment of rat brain microsomes resulted in the increase of binding constant of Con A to the microsomal surface without significant loss of binding sites. © 1998 Elsevier Science B.V.

Keywords: Concanavalin A; Mannoside; Mannosidase; Fluorescence polarization; Flow cytometry; Brain microsome

1. Introduction

A mannoside is a basic component of glycoproteins. Initially in the synthesis of glycoproteins the very long chain lipid, dolichol, is phosphorylated by dolichol kinase in endoplasmic reticulum and then mannose-*P*-dolichol is produced. This mannose–dolichol compound is utilized to form high-mannose type intermediates in the lumen side of the reticulum and finally the oligosaccharides are transferred to Asn residue of precursor peptide of glycoproteins. These glycopeptides are transported to Golgi-body and processed to form more complex sugar chains.

The oligosaccharides in glycoproteins thus produced play important roles in cell functions and cell-to-cell recognition. However, the role of oligosaccharide residues in synaptic neurotransmission is not known. Gurd and Fu [1] reported that concanavalin A receptors associated with rat brain synaptic junctions are high-mannose type oligosaccharides. Concanavalin A was used as a marker of synaptic vesicle recycling. This lectin could bind to rat brain synaptosomes and was taken up as observed by electron microscopy [2]. Moreover Scherer and Udin [3] reported that concanavalin A reduced habituation in the tectum of the frog through desensitization of

* Corresponding author. Fax: +81-975-86-6202; E-mail: xyosida@oita-med.ac.jp

PII S0005-2736(97)00268-X

glutamate receptors at the retinotectal synapse. These reports suggest that concanavalin A-reactive oligosaccharides on the synaptic membrane may play an important role in the synaptic functions.

Recently we have observed the change of characteristics of sialic acid in rat brain microsomes after the brightness-discrimination learning task depending on dietary fatty acids [4]. We showed that the neuronal activity itself in brain during the learning task modified the microsomal saccharide (or sialic acid) moieties. We needed to measure the change of the amount and characteristics of oligosaccharides in the small amount of microsomal membranes to address the mechanism of biochemical changes of the membrane surface by the neuronal activity.

The analysis of oligosaccharides of membrane components is normally time-consuming and a milligram-order of membrane proteins is necessary for precise analysis. In this report we show the fluorescence polarization technique for a microgram-order of microsomal proteins using fluorescein isothiocyanate (FITC)-labeled concanavalin A (Con A) and have presented that the alpha-mannosidase-treatment of microsomes resulted in the increase of the binding constant against Con A without significant loss of binding sites.

2. Materials and methods

2.1. Preparation of rat brain microsomes

Rat brain microsomes were prepared as reported previously [5] with slight modification. Rat cerebra were homogenized with glass–Teflon homogenizer in 5–6 volumes of buffer A (0.32 M Sucrose–10 mM Tris–HCl, 1 mM EDTA, pH 7.4). This homogenate was centrifuged at $1100 \times g$ for 5 min. The supernatant was centrifuged at $17{,}000 \times g$ for 10 min. The second supernatant was then centrifuged at $100{,}000 \times g$ for 40 min. The pellets (microsomal fraction) thus obtained were collected and suspended in buffer B (0.32 M Sucrose–10 mM Hepes, pH 7.5). FITC-labeled concanavalin A (Con A–FITC) from *Canavalia eusiformis* (FITC 3.4 mol/mol of Con A), FITC-labeled bovine serum albumin (BSA–FITC) (FITC 12 mol/mol of BSA) and alpha-mannosidase (α-D-Mannoside mannohydrolase; EC3.2.1.24) from Jack bean were purchased from Sigma Chemical (St. Louis, USA). The rat brain microsomes in 100 μl which contained 8–10 mg protein/ml were mixed with 4 μl of alpha-mannosidase (4 U/ml) and diluted to 0.5 ml with 100 mM sodium acetate buffer (pH 5.0). Then, the mixture was incubated at 37°C for 2 h. As a control the microsomes were mixed with 4 μl of water instead of alpha-mannosidase at ice-cold temperature. Both mixtures were diluted with buffer B to a volume of 2 ml and centrifuged at $100{,}000 \times g$ for 30 min. The microsomal pellets were resuspended in 200 μl of buffer B. The protein concentration was measured by the BCA (Pierce, USA) method.

2.2. Fluorescence measurements

Fluorescence polarization measurements were carried out using a fluorescence spectrometer, F4010 (Hitachi, Japan) attached with the automatic polarization system. A 150 W xenon lamp was used as a light source. Parallel and perpendicular polarized emission components of the fluorescence light were detected with excitation at 488 nm. The excitation band-pass was 3 nm and the emission band-pass was 10 nm, with the emission wavelength at 518 nm. The Con A–FITC was diluted to 0.98 μM in a total volume of 1 ml. The assay buffer was 0.32 M Sucrose–10 mM Hepes, pH 7.5 (buffer B). The samples were diluted to 10 μg protein/ml, and set in a square 10×10 mm quartz cell which was maintained at 26°C during measurements. An aliquot of Con A–FITC in 1 μl (at 0.98 μM) was successively added to the sample. Similarly, an aliquot of BSA–FITC with the same concentration of Con A–FITC on the basis of FITC concentration was added as a control experiment. Polarization was automatically measured six times at each titration point with an integration time of 10 s for each measurement, and the resulting polarization values were averaged. The polarization of fluorescence is defined as the difference between the parallel and perpendicular emission components, $I(_{//})$ and $I(_{\perp})$, respectively, with respect to the total intensity when vertically polarized excitation is used. The polarization is defined here as $P = (I(_{//}) - I(_{\perp}) * G)/(I(_{//}) + I(_{\perp}) * G)$, where G is the 'machine-constant' and automatically calculated before starting the measurement of samples.

2.3. Flow cytometry

Rat brain microsomes were diluted to 0.1 mg protein/ml and added with 13 pmol of Con A–FITC. As a control, microsomes were diluted and added with BSA–FITC in the same concentration as Con A–FITC on the basis of FITC concentration. The fluorescence emitted from Con A–FITC bound to the microsomes was analyzed by the flow cytometry (FACS Calibur, Becton Dickinson) equipped with a 15 mW air-cooled 488 nm argon laser. Forward and side scatter as well as fluorescence signals were acquired with an excitation wavelength at 488 nm. Acquisition and processing of data was carried out counting less than 10,000 'cells' or particles. Fluorescence measurements were done on a logarithmic scale. Results were obtained by gating on microsomal auto-fluorescence and examining the histograms of FL1-H (fluorescence emission height at 530 nm) of FITC conjugates with and without microsomes.

3. Results

When the polarization (P) values were plotted against the amount of added Con A–FITC as shown in Fig. 1, the difference was clear between the mannosidase-treated and untreated (control) microsomes. These plots of the polarization showed the binding profiles of Con A–FITC to the microsomal membranes, indicating that the polarization of free Con A–FITC is lower than that of the bound Con A–FITC. When the amount of added Con A–FITC is much less than that of binding sites (i.e., almost all Con A–FITC is in the bound form), the value P may be larger than 0.2 which was actually calculated by non-linear curve fitting method as described later. When the excess amount of Con A–FITC was added, the value P approaches to a constant (nearly 0.12) which should be close to the P value for the free Con A–FITC, but was not exactly the same as the P value of free Con A–FITC without microsomes, because the turbidity of microsomal suspension would affect the P value by depolarization of the scattered light. Fig. 1 shows that the mannosidase-treatment of microsomes decreased the polarization of the ligand (Con A–FITC) when compared with the control (without mannosidase). In order to analyze the binding characteristics from these restricted data set, we have to adopt a curve-fitting technique and evaluated the values of initial and the saturated points.

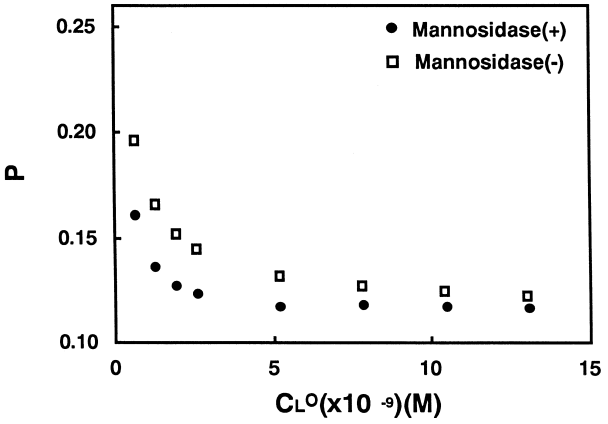

Fig. 1. Con A–FITC fluorescence polarization (P) values after incubation with rat brain microsomes with and without mannosidase treatment. The closed circles (●) and open squares (□) are for mannosidase treatment (mannosidase (+)) and for the control (mannosidase (−)), respectively. The P values at $C_L^O = 0$ in both cases were obtained by curve-fitting to the experimental data points. Details are described in Section 2.

Fig. 2 explains how to obtain the initial and the saturated P values using the equation,

$$Y = F(X) = X * c * (1 + 1/(a * (b - X)) \qquad (1)$$

for the binding analysis of a ligand to a binding site. See Appendix A for detailed explanation. In order to fit the experimental data to theoretical curves, the x (Con A) $- y$ (P) plots originally obtained were converted to X ($-P$) $- Y$ (Con A) plot which was presented in Fig. 2 as an example. This type of plot could be well fitted by the Eq. (1). In this figure, R is defined as saturation, C_{BL}/C_B^O, where C_{BL} is the concentration of bound Con A to binding sites and C_B^O is total concentration of Con A-binding sites in the assay mixture.

Fig. 3a shows a plot for binding of Con A–FITC to rat brain microsomes, where Y axis represents the concentration of FITC in Con A–FITC, and X axis represents minus P(polarization, $-P$) as shown in Fig. 2. In this figure, the P values at $C_L^O = 0$ were plotted, and these values were calculated by fitting the experimental data to the Eq. (1) with using non-linear regression analysis as presented in Fig. 2. Fig.

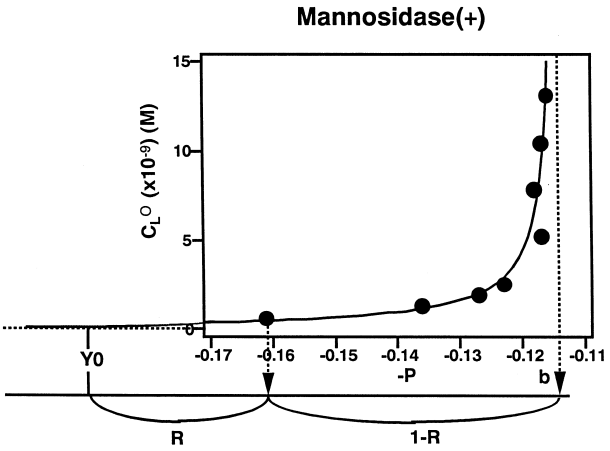

Fig. 2. Explanatory drawing for curve-fitting to the observed polarization (P) values. This explains how to obtain the initial and final (saturated) P values using the equation $Y = F(x) = x * c * (1 + 1/(a * b - a * x))$ for the binding analysis of a ligand to a binding site. The X axis of this graph represents $-P$ (minus P), in which P is shown in y-axis of Fig. 1, and the Y-axis represents C_L^O which is shown in x-axis of Fig. 1. R is defined as saturation, C_{BL}/C_B^O, where C_{BL} is the concentration of the bound form of Con A to the binding sites and C_B^O is the total concentration of Con A in the assay mixture. Yo represents the initial P value, and b represents the final (saturated) P value.

3b shows plots for binding of BSA–FITC to the control and mannosidase-treated microsomes. In the case of Con A–FITC (Fig. 3a), mannosidase-treated microsomes show smaller P values than the control microsomes. On the other hand, in the case of BSA–FITC (Fig. 3b), the mannosidase-treated microsomes show a little larger P values than the control microsomes. Even when increasing the amount of BSA–FITC up to 50×10^{-9} M, the P value was still far from saturation and it persisted to be decreasing. Fig. 3c shows plots for blank without microsomes and the P value of free Con A–FITC is nearly constant for various amount of the conjugate. The P values of free BSA–FITC increased with increasing the amount of BSA–FITC, suggesting the change of concentration-dependent aggregation or other conformation state of BSA–FITC.

Fig. 4a and b show modified Scatchard plots of C_L^O/R vs. $1/(1-R)$ for BSA–FITC and Con A–FITC, where R denotes the saturation as shown in Fig. 2. In this plot the slope represents the binding constant, and the intersection on the abscissa the concentration of binding sites (See Appendix A in detail). Fig. 4a shows that the binding constant of BSA–FITC for the mannosidase-treated microsomes was 1.72×10^9 (M^{-1}), and for the control was 3×10^9 (M^{-1}). The C_L^O in this plot represents the concentration of total BSA–FITC added in the incubation mixture. The binding constant for mannosidase-

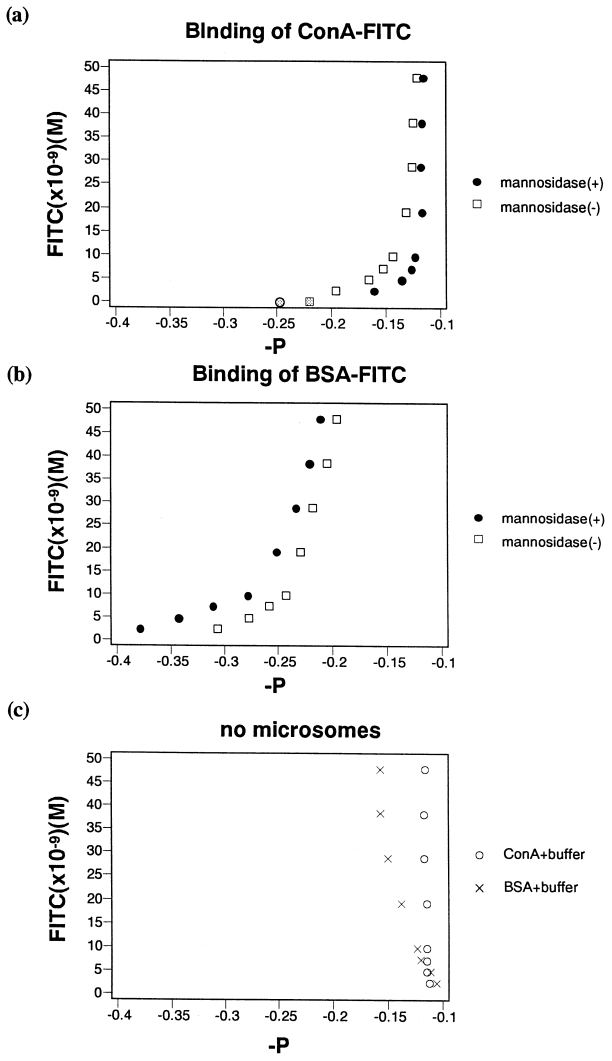

Fig. 3. Plots of $(-P)$ vs. C_B^O (concentration of FITC conjugates). The closed circles (●) and open squares (□) are for the mannosidase-treated (mannosidase (+)) and for the control (mannosidase (−)) microsomes, respectively. (a) The plot for the binding of Con A–FITC to rat brain microsomes. The shaded circle and shaded square are positioned at Y(FITC) = 0 at which the P values were calculated by curve-fitting to the experimental data points as shown in Fig. 2. (b) The plot for the binding of BSA–FITC to rat brain microsomes. (c) The plot for free Con A–FITC and BSA–FITC in the buffer without microsomes.

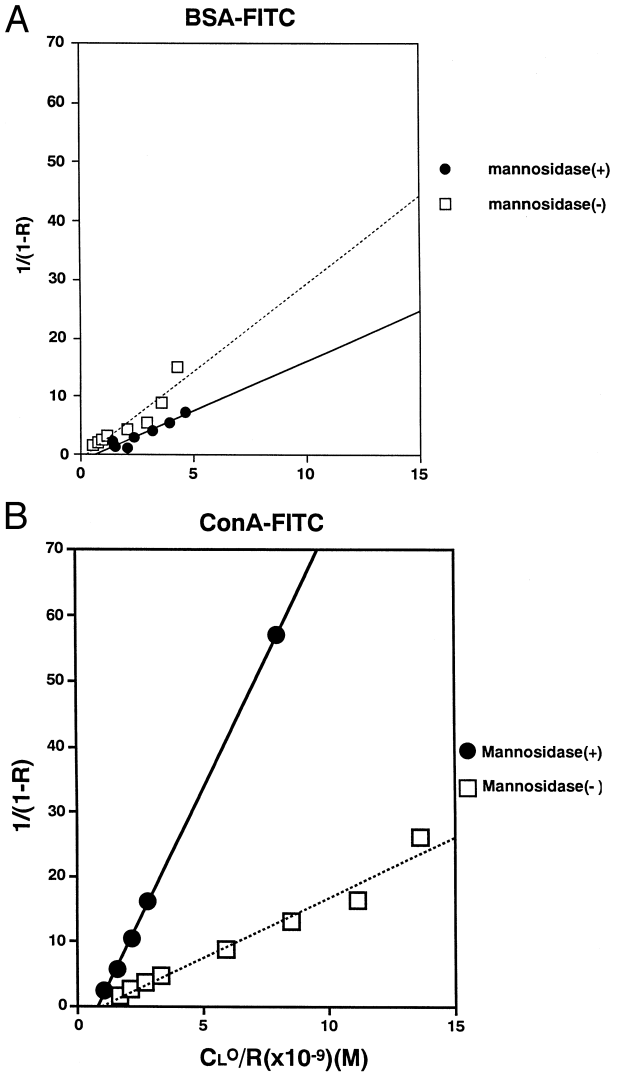

Fig. 4. Modified Scatchard plot for the binding of BSA–FITC (a) and Con A–FITC (b) to rat brain microsomes. The *Y*-axis represents $1/(1-R)$ and the *X*-axis C_L^O/R. The closed circles (●) and open squares (□) are for the mannosidase-treated (mannosidase (+)) and for the control (mannosidase (−)) microsomes, respectively. The solid line was fitted to the closed circles, and the dotted line was fitted to the open squares.

treated microsomes was almost the same as that of the control. This shows that non-specific binding occurred between microsomes and BSA–FITC. On the other hand, Fig. 4b shows that the binding constant of Con A to mannosidase-treated microsomes is larger than the control without significant loss of binding sites (C_B^O). From these plots, the binding constant, K, was calculated to be 7.93×10^9 (M^{-1}) for the mannosidase-treated microsomes, and 1.97×10^9 (M^{-1}) for the control; C_B^O was 0.82×10^{-9} (M) for mannosidase-treated microsomes and 0.85×10^{-9} (M) for the control. In summary, for the control microsomes, the binding constant of BSA–FITC (3×10^9) was not much different from that of Con A–FITC (2×10^9) and the concentration of binding site for BSA–FITC (0.27×10^{-9} M) was smaller than that for Con A–FITC(0.96×10^{-9} M). On the other hand, for the mannosidase-treated microsomes, the binding constant of BSA–FITC (1.7×10^9) was smaller than that of Con A–FITC (7.9×10^9) and the concentration of binding site for BSA–FITC (0.68×10^{-9} M) was not much different from that for Con A–FITC (0.81×10^{-9} M). These results indicate that the mannosidase-treatment increased the specific binding of Con A to saccharide residues on the microsomal membrane more than the non-specific binding. This also suggests that the mannosides or other saccharides with a relatively large binding constant to Con A were exposed after removal of mannosides with a weak binding to Con A by alpha-mannosidase.

In this fluorescence polarization technique, the detection of binding of Con A–FITC conjugate to the membrane surface is based on the change of FITC fluorescence intensity upon binding of Con A to oligosaccharide (mainly mannosides). The evidence that the polarization of fluorescence decreased when free Con A–FITC concentration was increased suggests that upon binding of Con A–FITC to the membrane surface the rotational mobility of FITC may become restricted, indicating that FITC on Con A became interacted with some membrane components upon binding of Con A–FITC to the membrane surface. This idea is supported by the data shown in Fig. 5 measured by flow cytometry. Fig. 5a shows the flow cytometric patterns of BSA–FITC in the presence and absence of excess amount of microsomal membranes. In this case the pattern in the presence of microsomes was almost the same as that in the absence of microsomes and the subtracted pattern ([+microsomes] minus [control]) was small. This indicates that the fraction of the bound form of BSA–FITC is small when comparing with the free form. However, the shift of peak position in the histogram was noticed for the bound form (subtracted). Fig. 5b shows the flow cytometric patterns

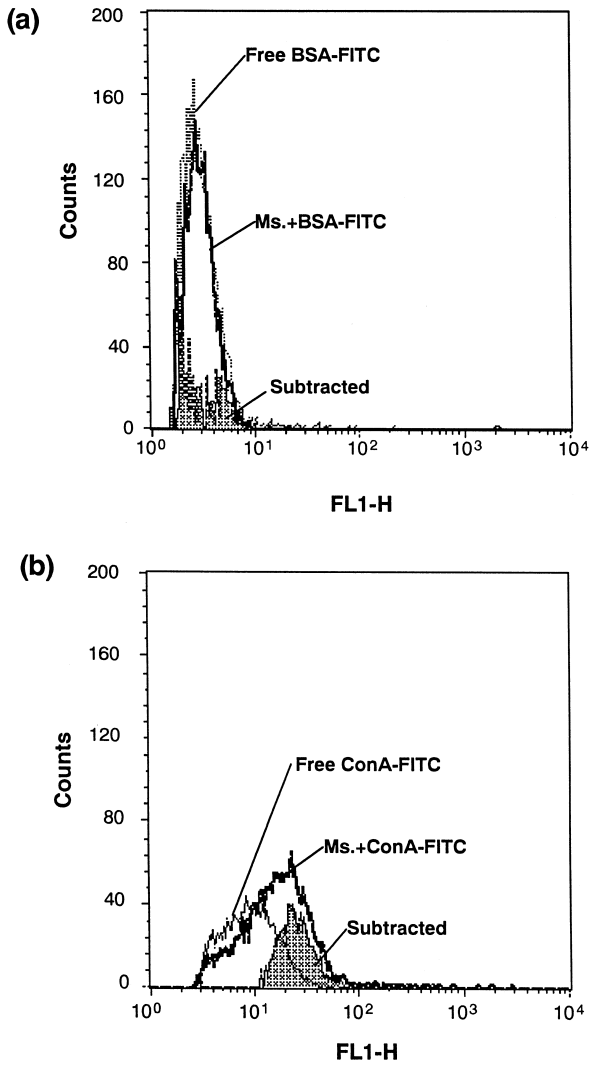

Fig. 5. Flow cytometric patterns of BSA–FITC and Con A–FITC in the presence and absence of excess amount of microsomal membranes (see Section 2). (a) BSA–FITC represents free form of BSA–FITC, and [Ms. + BSA–FITC] represents the BSA–FITC in the presence of the microsomal membranes. The subtracted trace ([Ms. + BSA–FITC] − [free BSA–FITC]) is shown in the shaded area denoted as 'Subtracted'. (b) Con A–FITC represents free Con A–FITC, and [Ms. + Con A–FITC] represents the Con A–FITC in the presence of the microsomal membranes. The subtracted trace ([Ms. + Con A–FITC] − [free Con A–FITC]) is shown in the shaded area. The background fluorescence from the buffer and microsomes (auto-fluorescence) was removed by subtracting the buffer fluorescence (very small) from the free FITC conjugates and the microsomal autofluorescence from the 'Ms. + FITC conjugate'.

of Con A–FITC in the presence and absence of excess amount of microsomal membranes. Without Con A–FITC the fluorescence of microsomal membrane itself (auto-fluorescence) was small (FL1-H was all below 5) (not shown in this figure). This auto-fluorescence components of microsomes and buffer solution were subtracted from the profile for BSA– or Con A–FITC in the presence of microsomes, and from the profile for free BSA– or Con A–FITC, respectively. The value of *x*-axis (FL1-H) is the fluorescence intensity of the particle detected in the fluorescence signal height by photomultiplier through bandpath-filter at ~530 nm. The subtracted histogram pattern shows that the bound Con A–FITC to the membrane increased in its fluorescence intensity more than the free form as the histogram peak position was shifted clearly when compared with the profile for free Con A–FITC. This indicates that the physical moiety around the FITC was changed upon binding of Con A–FITC to the membrane surface and supports the idea that polarization change of Con A–FITC was caused by restriction of the mobility upon binding to the membrane surface mannosides.

4. Discussion

Oligosaccharides bound to lipids and proteins on cell membranes have many important functions in cell-to-cell recognition and signal transfer. In neurons, we are currently investigating a role of dietary fatty acids in regulating synaptic functions, and found that chemical moiety of sialic acid on membrane surface of brain microsomes was changed by dietary fatty acids and learning tasks [4]. During this study we have faced a problem on how to quantify the change of membrane surface oligosaccharide of small amount of organella. We, therefore, developed the analysis method to detect changes of oligosaccharide moiety of membranes in high sensitivity.

FITC-labeled concanavalin A (Con A–FITC) was used to quantify the binding of this lectin to mannosides using chromatographic methods [6]. This chromatographic technique was adopted to measure the binding constant of Con A–FITC to the mannosides, however, we could not use this method for the small amount of membrane fractions available.

On the other hand, fluorescence polarization technique has been used for detection of specific interaction between fluorophors and biomaterials. The bindings of fluorescence-labeled DNA fragments to pro-

teins [7,8] and of FITC-labeled IgG to anti-IgG antibody [9] were analyzed. This technique was not so far applied to Con A–FITC binding analysis to oligosaccharides. As this technique is highly sensitive and picomolar-order of samples could be revealed [9], we have applied this technique to the binding of Con A–FITC to the microsomal membrane surface. We improved the analysis (curve-fit) method to obtain the initial and final (saturated) polarization values which otherwise could not be obtained experimentally. We have presented the analysis procedure in this paper and only a modified Scatchard analysis after obtaining R (saturation) values was shown in Fig. 3. From this analysis we could obtain the binding constant and the binding-site concentration in the assay mixture. We could obtain directly those factors from the non-linear curve fitting (not shown in this paper), and the values obtained from both procedures are quite consistent.

We speculated that the change of polarization of Con A–FITC fluorescence upon binding to the membrane surface oligosaccharides (mannosides) was caused by the change of chemical or physical moiety of FITC. This change of moiety (hydrophobic or hydrophilic) around the fluorescent probe may affect the fluorescence intensity by changing the quantum yield of the fluorescent and this is confirmed by the flow cytometric analysis as shown in Fig. 5. With this flow cytometric method, the free and bound form of Con A–FITC could be separately detected, and actually the fluorescence intensity of the bound form was larger than the free form. The increase of fluorescence intensity of Con A–FITC bound to isolated Golgi fractions from rat liver was reported by Guasch et al. [10]. Weak or non-specific binding of BSA–FITC conjugate to the membrane showed only a small increase of fluorescence intensity. This suggests that only the specific binding of FITC conjugate to the membrane modifies significantly the chemical or physical environment of the fluorescent probe and this modification would lead to the steric hindrance of motion of the probe. The reason why the P value (> 0.3) of bound-form of BSA–FITC is larger than that (< 0.25) of Con A–FITC is not known at present. As the P value of the free form of BSA–FITC is not much different from the free form of Con A–FITC, that difference of membrane-bound BSA–FITC polarization may be caused by the specific interaction between the FITC and the binding site of the membrane.

How does the treatment of microsomes by alpha-mannosidase increase the binding constant of Con A–FITC to the microsomes? By the mannosidase-treatment a part of oligosaccharides on the surface of microsomal membranes may be removed and then the rest of core mannosides which had larger affinity to Con A than the removed oligosaccharides were readily accessible to Con A–FITC. The high-affinity mannosides to Con A might be positioned at the site near the lipid surface (or possibly 'core site' of glyco-conjugates) of the membrane and their accessibility to Con A–FITC might be lowered in the control microsomes possibly by the steric hindrance from other oligosaccharides which may be removed by the mannosidase-treatment under the condition described above. This is a plausible explanation for the present, rather unexpected, observation that the mannosidase had induced the increase of binding constant of Con A against the microsomes without change of the binding site concentration. Baenziger and Fiete [11] reported that sequential removal of peripheral sugars on branches arising from position C-2 of the alpha-linked mannose residues of glycopeptides resulted in a progressive increase in the association constants for the core structure.

In conclusion we have shown that the fluorescence polarization technique was useful to obtain the binding factors of Con A to the small amount of membrane fractions. We measured the change of binding constant and the concentration of binding sites of rat brain microsomes with and without alpha-mannosidase-treatment. We observed the increase of binding constant without significant change of binding sites after the treatment. The application of this technique to detect the neuronal activity-associated changes of membrane surfaces of brain microsomes is now under progress.

Appendix A. Equations for binding assay

In the binding of a ligand (L) to a receptor (B) (i.e., B + L ↔ BL), the binding constant, K, is written in:

$$K = C_{BL}/C_B * C_L = C_{BL}/\left(\left(C_B^O - C_{BL}\right) * C_L\right)\ldots, \quad (1A)$$

where C_{BL} is the concentration of bound-form of the receptor with the ligand, C_B is the free form of the receptor, C_B^O is the total concentration of the receptor which is capable to bind with the ligand, and C_L is the concentration of free ligand (not bound to the receptor). When $X = C_{BL}/C_B^O$ (which is the same meaning as R, the saturation, as described below) and $Y = C_{BL} + C_L$ were set, Y is the total ligand concentration. This setting is adopted for curve-fitting using simple equation:

$$K = \left(C_{BL}/C_B^O\right)/\left(\left(1 - C_{BL}/C_B^O\right) * C_L\right)$$
$$= X/\left((1 - X) * \left(Y - X * C_B^O\right)\right).$$

This is modified to:

$$Y = X * C_B^O * \left(1 + 1/\left(K * C_B^O * (1 - X)\right)\right) \ldots \quad (2A)$$

The curve-fitting equation is set to:

$$F(X) = X * c * (1 + 1/(a * (b - X))), \quad (3A)$$

(same as Eq. (1) in the text)where $a = K * C_B^O$, $c = C_B^O$, and b is the maximum (saturated) value of X (when X is normalized ($0 \le X \le 1$), b should be 1). As X should represent the values related to P (polarization) values experimentally and is not normalized, b must be a variable factor. When a curve-fitting is performed using Eq. (3A) varying factors a, b, and c, the quasi-Newton fitting algorithm was used to minimize the sum of squares error (SSE). The program, MacCurveFit (ver. 1.2) on Macintosh written by Kevin Raner, Australia, was mainly used for this task.

Actually the extent of saturation (R) of ligand binding is calculated at each concentration of added ligand after obtaining the maximum level of binding and the initial value (when $C_L^O = 0$), where C_L^O is the total concentration of ligand. In the present polarization assay, however, the initial value of the polarization of Con A–FITC fluorescence can not be measured experimentally as the fluorescence should be zero when $C_L^O = 0$, and in this case the initial value of the polarization should be obtained by extrapolation from the observed values with a curve-fitting technique described above. In this polarization measurement as shown in Fig. 1, the values of x-axis (C_L^O) were transferred (rotated to left) to Y-axis and the values of y-axis (P) were to X-axis, then the curve-fitting using Eq. (3A) was performed to calculate the intersection of X-axis ($(1 + a * b)/a$), which is equal to the 'initial polarization' value. The value of b in Eq. (3A) is the saturated point of X (P) and is obtained by the curve-fitting.

In the Scatchard (modified) analysis, we can change Eq. (1A) to;

$$C_{BL}/C_B = K * \left(C_L^O - C_{BL}\right) \ldots, \quad (4A)$$

where C_L^O is total concentration of ligand.

When R is defined as the extent of saturation,

$$R = C_{BL}/C_B^O \text{ and } (1 - R) = C_B/C_B^O.$$

Then the formula (Eq. (4A)) is changed to:

$$1/(1 - R) = K * \left(C_L^O/R - C_B^O\right) \ldots \quad (5A)$$

When plotting $1/(1 - R)$ vs. C_L^O/R, the slope of the fitted line corresponds to K (binding constant) and the intersection point with X-axis corresponds to C_B^O according to Eq. (5A).

References

[1] J.W. Gurd, S.C. Fu, J. Neurochem. 39 (1982) 719–725.
[2] P.R. Gordon-Weeks, D.H. Hones, Proc. R. Soc. Lond. B219 (1983) 413–422.
[3] W.J. Scherer, S.B. Udin, Brain Res. 667 (1994) 209–215.
[4] S. Yoshida, M. Miyazaki, M. Takeshita, S. Yuasa, T. Kobayashi, S. Watanabe, H. Okuyama, J. Neurochem. 68 (1997) 1269–1277.
[5] S. Yoshida, M. Takeshita, Arch. Biochem. Biophys. 254 (1987) 170–179.
[6] M. Sarkar, G.C. Majumder, T. Chatterjee, Biochim. Biophys. Acta 1070 (1991) 198–204.
[7] T. Heyduk, J.C. Lee, Proc. Natl. Acad. Sci. 87 (1990) 1744–1748.
[8] V. LeTilly, C.A. Royer, Biochemistry 32 (1992) 7753–7758.
[9] M. Tsuruoka, E. Tamiya, I. Karube, Biosensors and Bioelectronics 6 (1991) 501–505.
[10] R.M. Guasch, C. Guerri, J.E. O'Conner, Exp. Cell Res. 207 (1993) 136–141.
[11] J.U. Baenziger, D.J. Fiete, J. Biol. Chem. 254 (1979) 2400–2407.